

Self-assembled nanostructures with tridentate cyclometalated platinum(II) complexes†

Wei Lu, V. A. L. Roy and Chi-Ming Che*

Received (in Cambridge, UK) 25th May 2006, Accepted 28th June 2006

First published as an Advance Article on the web 4th August 2006

DOI: 10.1039/b607422g

Self-assembly of positively charged and charge-neutral tridentate cyclometalated platinum(II) complexes leads to nanowires and the drop-cast film containing these nanowires behaves as a n-type semiconductor.

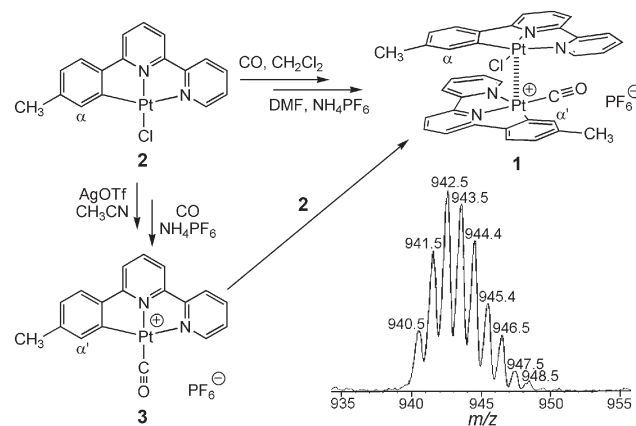
Metal-based quasi-one-dimensional structures derived from metal-philic Pt··Pt interactions, such as Magnus' green salt [Pt(NH₃)₄][PtCl₄]¹ and Krogmann's salt [K₂Pt(CN)₄Br_{0.3}](H₂O)_{*n*},² have long been known. The overlapping of the 5d_{z²} orbitals of Pt(II) ions not only renders these types of solids deep-colored but also confers to them conducting³ and sensing⁴ capabilities. Recently, a microfilament of [Pt(NH₂R)₄][PtCl₄] (R is an alkyl group) was made by electro-spinning and found to be a p-type semiconductor.⁵ Studies have also revealed that some square-planar Pt(II) complexes with aromatic α -diimine and/or cyclometalating ligands can aggregate in the solid state⁶ or in non-polar solvents⁷ through Pt··Pt and/or π - π interactions. In recent years, one-dimensional nanostructures of organic molecules⁸ and metal complexes⁹ have been reported to have properties distinct from their bulk materials. In this context, nanostructured materials combining a rigid metal-ligand coordination framework and extended aromatic π -conjugation are, to our best knowledge, unprecedented. We communicate herein the one-dimensional nanostructures that self-assembled from the heteroleptic binuclear Pt(II) complex $\{[(C^{\wedge}N^{\wedge}N)PtCl][[(C^{\wedge}N^{\wedge}N)PtC=O](PF_6)\}$ (**1**, HC[^]N[^]N = 6-(4'-methylphenyl)-2,2'-bipyridine). Solution-processible nanostructured films of this compound exhibit n-type semiconducting behavior in a bottom-contact TFT (thin-film field-effect transistor) configuration.

Bubbling CO gas into a solution of $[(C^{\wedge}N^{\wedge}N)PtCl]$ (**2**)¹⁰ in CH₂Cl₂ gave a dark green precipitate which is sparsely soluble in common organic solvents including DMF (dimethylformamide) and DMSO (dimethylsulfoxide). Sonication of this solid in DMF in the presence of NH₄PF₆ resulted in a dark red solution. Addition of water into the DMF solution precipitated a deep blue solid. The ¹H NMR spectra show two sets of signals with a 1 : 1 integration ratio, corresponding to two chemically non-equivalent (C[^]N[^]N) ligands. Only one C=O signal at 206 ppm and one C=O stretching at 2094 cm⁻¹ were found in the ¹³C NMR and IR (KBr pellet) spectra, respectively. The electrospray ionisation (ESI) MS spectrum shows three clusters of peaks with maximum at *m/z* 468.1, 942.5 (Scheme 1) and 1418.1 (weak) whose values and

isotopic patterns correspond to the $[(C^{\wedge}N^{\wedge}N)PtC=O]^+$, $\{[(C^{\wedge}N^{\wedge}N)PtCl][[(C^{\wedge}N^{\wedge}N)PtC=O]]^+$ and $\{[(C^{\wedge}N^{\wedge}N)PtCl]_2-[(C^{\wedge}N^{\wedge}N)PtC=O]\}^+$ species, respectively. These data lead us to propose a heteroleptic binuclear structure for this compound (**1**), as shown in Scheme 1.

We thus prepared $[(C^{\wedge}N^{\wedge}N)PtC=O](PF_6)$ (**3**) by treating **2** with AgOTf before CO bubbling and anion exchange.¹⁰ A C=O stretching at 2109 cm⁻¹ was found in the IR (KBr pellet) spectrum of **3**, which is 15 cm⁻¹ higher than that for **1**. Mixing **2** and **3** in 1 : 1 molar ratio in CH₃CN or DMSO gave a dark red solution. The color change in this reaction was depicted with UV-vis absorption spectra as shown in Fig. 1. The difference UV-vis absorption spectrum (Fig. 1, inset) between the chemical mixture and mathematical summation of **2** and **3** shows an absorption band at $\lambda_{max} \sim 510$ nm, indicating the formation of a new species. Removing the solvent gave a dark blue solid with identical spectroscopic features to **1**. All the aromatic proton signals in the ¹H NMR of **1** are shifted towards the higher field when compared with their respective counterparts in **2** and **3**. Typically, the singlet α -H of **2** and α' -H of **3** (see Scheme 1 for labeling) shift (in *d*₆-DMSO) from 7.28 and 6.81 ppm to 6.70 and 6.30 ppm in **1**, respectively. This supports the idea that **1** consists of $[(C^{\wedge}N^{\wedge}N)PtCl]$ and $[(C^{\wedge}N^{\wedge}N)PtC=O](PF_6)$ fragments in a 1 : 1 molar ratio and these two planar moieties are in a stacking geometry, most likely being linked by Pt··Pt interactions. While both **2** and **3** are orange in color and emissive in the solid state, **1** is deep blue in the solid state and non-emissive even at 77 K.

The UV-vis absorption spectrum of **1** in acetone is dependent on its concentration (Fig. 2). With concentration of **1** higher than 8.0×10^{-4} M, a distinct band with λ_{max} at 612 nm (an indicator of infinite Pt-based chain-like backbone)^{6,7} developed. Transmission



Scheme 1 Synthetic routes and ESI mass spectrum of **1**.

Department of Chemistry and HKU-CAS Joint Laboratory on New Materials, The University of Hong Kong, Pokfulam Road, Hong Kong SAR, China. E-mail: cmche@hku.hk; Fax: +852 2857 1586; Tel: +852 2857 2154

† Electronic supplementary information (ESI) available: Detailed synthesis and characterization data, additional UV-vis absorption spectra and TEM and SEM images. See DOI: 10.1039/b607422g

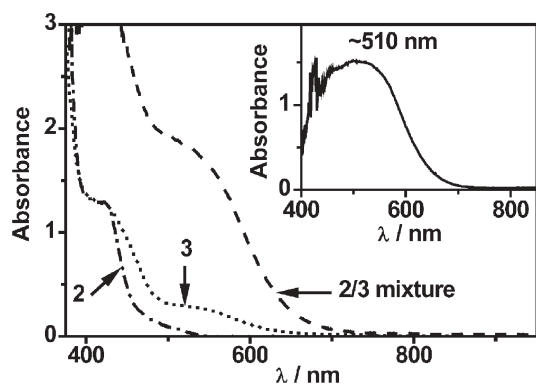


Fig. 1 UV-vis absorption spectra of **2**, **3** and a mixture of **2** and **3** (1 : 1 molar ratio) in DMSO; concentrations of **2** and **3** are 7.6×10^{-3} M in all these solutions; all these spectra were recorded using 1 mm cuvette. Inset shows the difference spectrum between the chemical mixture and mathematical summation of **2** and **3**.

electron microscopy (TEM) (Fig. 3a) and scanning electron microscopy (SEM) (Fig. 3b) images of the dispersion in acetone with a concentration of 6×10^{-3} M illustrated that the blue color comes from nanowires with a uniform diameter of ~ 30 nm and length extending over 10 μ m. Electron diffraction rings in the selected area electron diffraction (SAED) pattern (Fig. 3a, inset) indicated that there are two *d*-spacings, 3.38 and 6.84 Å, in the crystal packing of these nanowires. We note that the green complex [(terpy)Pt(C \equiv CC \equiv CH)](OTf) has a linear metal-based backbone with Pt \cdots Pt contact of 3.37 Å.⁷ The blue color of the nanowire dispersion derived from **1** disappeared upon addition of AgOTf salt or PPh₃ solid, both of which are known to remove chloride from the [(C \wedge N \wedge N)PtCl] fragment and thus destroy the charge balance in **1**.¹⁰ Complexes **2** and **3** alone did not form blue-colored nanowires under the same conditions. The Pt \cdots Pt

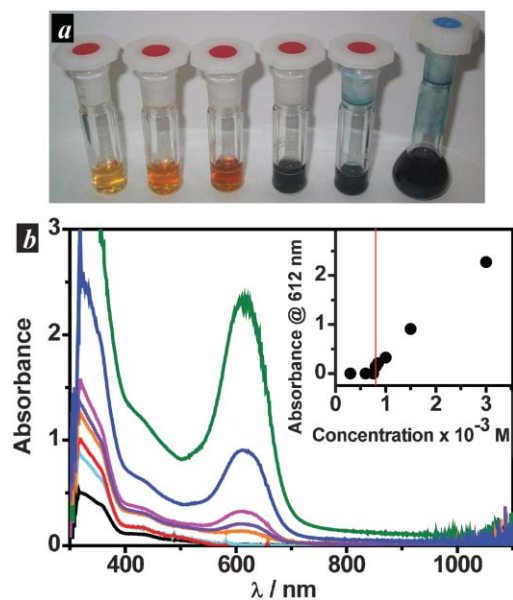


Fig. 2 (a) Solutions of **1** in acetone with various concentrations (from left, 0.30 , 0.60 , 0.75 , 1.5 , 3.0 and 6.0×10^{-3} M). (b) UV-vis absorption spectra of **1** in acetone with the concentration ranging from 3.0×10^{-4} to 3.0×10^{-3} M. Inset shows the plot of the absorbance at 612 nm against the concentration of **1**. All the spectra were recorded using 1 mm cuvette.

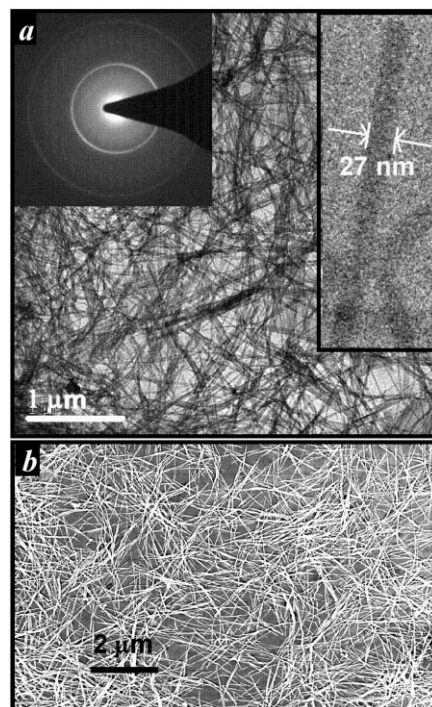


Fig. 3 (a) TEM and (b) SEM images of **1** dispersed in acetone with a concentration of 6.0×10^{-3} M. The right inset in (a) shows a nanowire with a diameter of 27 nm and the left inset in (a) shows the SAED pattern of these nanowires.

interaction is suggested to play a key role to direct the anisotropic growth of nanostructures. A concentration of **1** of higher than 8.0×10^{-4} M is critical for the growth of nanowires and the formation of an aggregation nucleus is the rate-determining step for the self-assembly kinetics.

These nanowires can also be prepared *in situ*.[‡] Sonicating a suspension of **2** and **3** (1 : 1 molar ratio, the concentration of **2** and **3** should be higher than 8.0×10^{-4} M) in acetone gave a deep blue dispersion of nanowires. These nanowires can be further dispersed into cyclohexane, toluene, Et₂O, MeO^tBu or water. Typically, 100 μ L of an acetone dispersion (6.0×10^{-3} M) was injected into 10 mL of these solvents and the resulting suspension was sonicated for 1 min to give a transparent blue dispersion (Fig. 4a) with the lowest absorption peak maximum in the 604–615 nm range. TEM and SEM (Fig. 4b) images of these dispersions revealed nanorods with a uniform diameter of ~ 30 nm and lengths spanning over 300 nm. Thus dilution and sonication can shorten the lengths of the nanowires but leave the diameter untouched.

Nanowires of **1** dispersed in acetone can be drop-cast on the top of a silicon substrate to form a self-assembled nanostructured film. The X-ray diffraction (XRD) pattern (Fig. 5a) revealed the good crystallinity of this film. The SEM image of the surface of a bottom-contact TFT device (Fig. 5c) with as-deposited nanowires is shown in Fig. 5b. The film consisted of randomly arrayed and overlapped nanowires with an average diameter of ~ 40 nm and an in-planar orientation. The output (I_{DS} vs. V_{DS} at various V_G , D, S and G denote drain, source and gate electrodes of the device, respectively, Fig. 5d) and transfer (I_{DS} vs. V_G at $V_{DS} = 40$ V) characteristics (see Supplementary Information[†]) of this device revealed that the nanostructured film behaves as an n-type semiconductor.¹¹ An appreciable source–drain current was

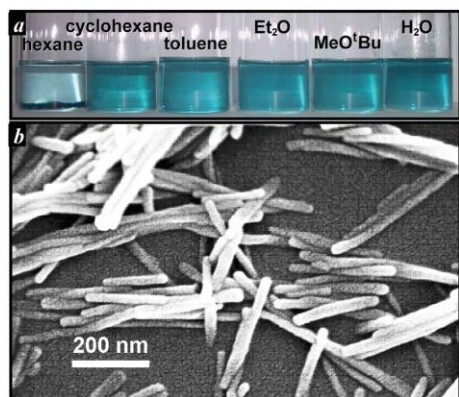


Fig. 4 (a) Dispersions of **1** in various solvents with concentrations being 6.0×10^{-5} M. (b) SEM image of **1** dispersed in MeO'Bu with a concentration of 6.0×10^{-5} M.

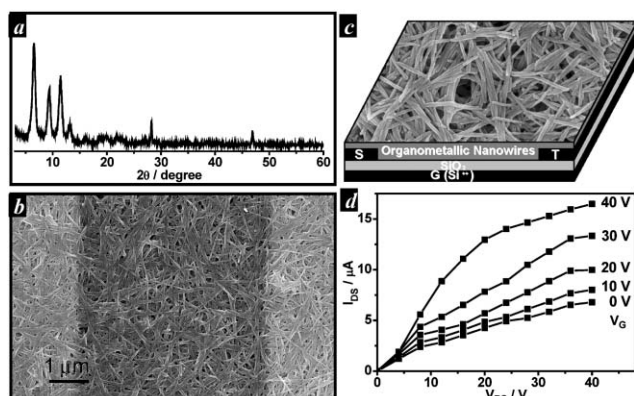


Fig. 5 (a) XRD pattern of a film made by drop-casting a 3.0×10^{-3} M dispersion of **1** in acetone on a silicon wafer. (b) SEM image of the surface of a bottom-contact TFT device (schematic drawing in Fig. 5c) with nanostructured **1** as semiconductor. (d) Output (I_{DS} vs. V_{DS}) characteristics of this TFT device.

observed even at $V_G = 0$ V, which may arise from the charged nature of the nanowires and the bulk conduction between the source and drain electrodes. Nevertheless, from the output curves, the field-effect electron mobility (μ_e) was calculated up to $10^{-2} \text{ cm}^2 \text{ V}^{-1} \text{ s}^{-1}$ at the saturation regime. Thus **1** belongs to the few examples of transition metal complex-based semiconductors for TFT applications.^{5,12} We note that nanostructured films containing low-dimensional inorganic semiconductors have been recently reported to possess tunable charge-transporting properties in TFT performance.¹³

The self-aggregation between charge-neutral and positively charged Pt(II) species through Pt··Pt and/or ligand–ligand interactions has proved to be a useful method for the preparation of organoplatinum-based nanowires. Recent studies also established the formation of one-dimensional nanowires from a neutral [Pt(CN-*t*Bu)₂(CN)₂] complex.¹⁴ Preliminary studies have been carried out and shown that the chemistry reported in the current work can tolerate various functional groups on the (C[^]N[^]N) ligands, which will be reported in due course.

This work was supported by the Strategic Research Themes on ‘Bio-nanotechnology’, ‘Organic Optoelectronics’ and ‘Nanotechnology Research Program’ of the University Development

Fund of The University of Hong Kong, Croucher Foundation, and the Hong Kong Research Grants Council (HKU 7039/03P). W.L. thanks The University of Hong Kong for a University Postdoctoral Fellowship. We thank Dr Stephen Sin-Yin Chui and Dr Kwan-Ming Ng for performing the XRD and ESI-MS measurements, respectively. Special thanks go to Mr Frankie Yu-Fee Chan and Mr Wing-Sang Lee in the Electron Microscopy Unit of The University of Hong Kong for technical assistance.

Notes and references

‡ Two methods were applied to prepare complex **1**. *Method I (serendipitous approach)*: to a solution of **2** (120 mg, 0.25 mmol) in CH_2Cl_2 (120 mL) was bubbled CO gas for 20 min. The resulting dark green solid was collected on a sinter-glass filter and washed thoroughly with CH_2Cl_2 and Et_2O . The solid (75 mg) was dissolved with DMF (1.5 mL) in the presence of NH_4PF_6 (20 mg). The resulting dark red solution was filtered with water (30 mL) to give a dark blue precipitate which was collected on a sinter-glass filter and washed thoroughly with water, CH_3OH , CH_2Cl_2 and Et_2O . Yield: 48% based on **2**. *Method II (rational approach)*: the mixture of **2** (19.0 mg, 0.04 mmol) and **3** (24.5 mg, 0.04 mmol) in CH_3CN (5 mL) was stirred for 10 min. The resulting red solution was filtered and evaporated to dryness to give a dark blue solid which was collected on a sinter-glass filter and washed thoroughly with CH_3OH , CH_2Cl_2 and Et_2O . Yield: >80%. See Supplementary Information for experimental details.†

- 1 G. Magnus, *Ann. Chim. Phys.*, 1829, **40**, 110.
- 2 K. Krogmann, *Angew. Chem., Int. Ed. Engl.*, 1969, **8**, 35.
- 3 J. M. Williams, *Adv. Inorg. Chem. Radiochem.*, 1983, **26**, 235; J. K. Bera and K. R. Dunbar, *Angew. Chem., Int. Ed.*, 2002, **41**, 4453.
- 4 C. E. Buss, C. E. Anderson, M. K. Pomije, C. M. Lutz, D. Britton and K. R. Mann, *J. Am. Chem. Soc.*, 1998, **120**, 7783.
- 5 W. R. Caseri, *Adv. Mater.*, 2003, **15**, 125.
- 6 R. J. Osborn and D. Rogers, *J. Chem. Soc., Dalton Trans.*, 1974, 1002; W. B. Connick, R. E. Marsh, W. P. Schaefer and H. B. Gray, *Inorg. Chem.*, 1997, **36**, 913 and references therein.
- 7 V. W. W. Yam, K. M. C. Wong and N. Zhu, *J. Am. Chem. Soc.*, 2002, **124**, 6506.
- 8 For examples, see: H. Liu, Y. Li, S. Xiao, H. Gan, T. Jiu, H. Li, L. Jiang, D. Zhu, D. Yu, B. Xiang and Y. Chen, *J. Am. Chem. Soc.*, 2003, **125**, 10794; A. D. Schwab, D. E. Smith, C. S. Rich, E. R. Young, W. F. Smith and J. C. de Paula, *J. Phys. Chem. B*, 2003, **107**, 11339; Z. Wang, C. J. Medforth and J. A. Shelnutt, *J. Am. Chem. Soc.*, 2004, **126**, 15954; M. Morikawa, M. Yoshihara, T. Endo and N. Kimizuka, *J. Am. Chem. Soc.*, 2005, **127**, 1358.
- 9 For examples, see: J. A. A. W. Elemans, R. de Gelder, A. E. Rowan and R. J. M. Nolte, *Chem. Commun.*, 1998, 1553; M. Enomoto, A. Kishimura and T. Aida, *J. Am. Chem. Soc.*, 2001, **123**, 5608; L. Valade, H. Casellas, S. Roques, C. Faulmann, D. de Caro, A. Zwick and L. Ariès, *J. Solid State Chem.*, 2002, **168**, 438; J. J. Chiu, C. C. Kei, T. P. Perng and W. S. Wang, *Adv. Mater.*, 2003, **15**, 1361(a); H. Liu, Q. Zhao, Y. Li, Y. Liu, F. Lu, J. Zhuang, S. Wang, L. Jiang, D. Zhu, D. Yu and L. Chi, *J. Am. Chem. Soc.*, 2005, **127**, 1120.
- 10 S. W. Lai, H. W. Lam, W. Lu, K. K. Cheung and C. M. Che, *Organometallics*, 2002, **21**, 226; W. Lu, B. X. Mi, M. C. W. Chan, Z. Hui, N. Zhu, S. T. Lee and C. M. Che, *J. Am. Chem. Soc.*, 2004, **126**, 4958; W. Lu, M. C. W. Chan, N. Zhu, C. M. Che, C. N. Li and Z. Hui, *J. Am. Chem. Soc.*, 2004, **126**, 7639.
- 11 C. D. Dimitrakopoulos and P. R. L. Malenfant, *Adv. Mater.*, 2002, **14**, 99; C. R. Newman, C. D. Frisbie, D. A. da Silva Filho, J.-L. Brédas, P. C. Ewbank and K. R. Mann, *Chem. Mater.*, 2004, **16**, 4436.
- 12 Z. Bao, A. J. Lovinger and J. Brown, *J. Am. Chem. Soc.*, 1998, **120**, 207; Y. Y. Noh, J. J. Kim, Y. Yoshida and K. Yase, *Adv. Mater.*, 2003, **15**, 699; S.-i. Noro, H.-C. Chang, T. Takenobu, Y. Murayama, T. Kanbara, T. Aoyama, T. Sassa, T. Wada, D. Tanaka, S. Kitagawa, Y. Iwasa, T. Akutagawa and T. Nakamura, *J. Am. Chem. Soc.*, 2005, **127**, 10012 and references therein.
- 13 B. Sun and H. Sirringhaus, *Nano Lett.*, 2005, **5**, 2408; D. V. Talapin and C. B. Murray, *Science*, 2005, **310**, 86.
- 14 Y. Sun, K. Ye, H. Zhang, J. Zhang, L. Zhao, B. Li, G. Yang, B. Yang, Y. Wang, S. W. Lai and C. M. Che, *Angew. Chem., Int. Ed.*, 2006, **45**, DOI: 10.1002/anie.200601588.